Published in final edited form as:
Exp Eye Res. 2010 November ; 91(5): 652–659. doi:10.1016/j.exer.2010.08.011.

Transduction of the inner mouse retina using AAVrh8 and AAVrh10 viaintravitreal injection

Thomas J. Giove[*], **Miguel Sena-Esteves**[§,#], and **William D. Eldred**[*]

[*] Laboratory of Visual Neurobiology, Boston University, Department of Biology, 5 Cummington St, Boston, MA 02215, P: 617-353-2439, F: 617-358-1124

[§] Department of Neurology, Massachusetts General Hospital, and Neuroscience Program, Harvard Medical School, Boston, MA 02129

Abstract

Adeno-associated virus (AAV) is a proven, safe and effective vector for gene delivery in the retina. There are over 100 serotypes of AAV, and AAV2 through AAV9 have been evaluated in the retina. Each AAV serotype has different cell tropism and transduction efficiency. Intravitreal injections of AAV into the eye tend to transduce cells in the ganglion cell layer (GCL), while subretinal injections tend to transduce retinal pigment epithelium and photoreceptors. Efficient transduction of the inner retina beyond the GCL is not well established with the current methodologies and serotypes used to date. In this study, we compared the cellular tropism of AAVrh8 and AAVrh10 vectors encoding enhanced green fluorescent protein (EGFP) using intravitreal injections. We found that AAVrh8 largely transduced cells in the GCL and also amacrine cells in the inner nuclear layer (INL), as well as Müller and horizontal cells. Inner retinal transduction with AAVrh10 was similar to AAVrh8, but AAVrh10 appeared to also transduce bipolar cells. The transduction efficiency as measured by the intensity of EGFP signal was 3.5 fold higher in horizontal cells transduced with AAVrh10 than AAVrh8. Glial fibrillary accessory protein (GFAP) levels were increased in Müller cells in transduced areas for both serotypes. The results of this study suggest that AAVrh8 and AAVrh10 may be excellent vector candidates to deliver genetic material to the INL, particularly for amacrine and horizontal cells, however they may also cause cellular stress as shown by increased glial GFAP expression.

Keywords

Adeno-associated virus; AAV; inner retina; inner nuclear layer; horizontal cells; retina; retinal gene delivery

Introduction

Adeno-associated virus (AAV) vectors have proven to be exceptionally efficient for *in vivo* gene delivery to several tissues (Grimm, 2002). More than 100 different AAV capsids have been cloned from human and non-human primates and a considerable number have been

Reprint requests to W.D. Eldred: eldred@bu.edu.
[#]Current Address: Department of Neurology and Gene Therapy Center, University of Massachusetts Medical School, Worcester, MA 01605

engineered to pseudotype AAV2 vectors (Surace and Auricchio, 2008). Some of the newer serotypes have shown exceptional efficiency for *in vivo* gene delivery to certain tissues, e.g. AAV8 in brain (Broekman et al., 2006; Klein et al., 2006) and liver (Wang et al., 2005), and AAV9 in brain (Cearley and Wolfe, 2006) and heart (Inagaki et al., 2006; Pacak et al., 2006).

The retina has been a particularly attractive target for viral-mediated gene-therapy owing to its relatively small isolated environment, which facilitates specific delivery of therapeutic agents to that tissue, as well as an immune-privileged environment which shields it from the rest of the body (Allocca et al., 2006; Martin et al., 2002). For example, several studies have demonstrated the efficacy of AAV-mediated gene therapy for treating Leber congenital amaurosis (LCA) in various animal models, including non-human primates (Bennicelli et al., 2008; Jacobson et al., 2006; Pawlyk et al., 2005). In fact, subretinal injection of AAV vectors has shown great promise in several concluded phase I clinical studies in LCA patients (Bainbridge et al., 2008; Cai et al., 2009; Cideciyan et al., 2008; Hauswirth et al., 2008; Maguire et al., 2008).

AAV1 through 9 vectors have been tested for their transduction properties in the retinas of rodents and primates (Auricchio et al., 2001; Lebherz et al., 2008; Rabinowitz et al., 2002; Yang et al., 2002). AAV2 and AAV5 have been used extensively in the retina and have proven effective for gene delivery to photoreceptors, retinal pigment epithelium cells (RPE) and ganglion cells (Allocca et al., 2006; Dinculescu et al., 2005). AAVrh8 and AAVrh10 are two additional AAV capsids isolated from rhesus monkey (Gao et al., 2003), and recombinant vectors using these capsids have yet to be tested in retina. Generally, intravitreal injections of AAV vectors lead to transduction of ganglion cells while subretinal injections lead to transduction of photoreceptors and RPE. We undertook this study to identify new AAV vectors capable of efficiently transducing additional retinal cell types for use as new tools to rapidly manipulate the molecular properties of these cells for future functional studies. In this brief report, we evaluated the cellular tropism of AAVrh8 and AAVrh10 vectors encoding enhanced green fluorescent protein (EGFP) in the mouse retina after intravitreal delivery. We also assessed potential negative effects of the resultant transductions by observing changes in glial fibrillary accessory protein (GFAP) expression in retinal Müller cells.

Materials & Methods

All reagents were purchased from Fisher Scientific (Waltham, MA) or Sigma (St. Louis, MO) unless otherwise indicated.

Animals

Adult, CD1 and C57BL/6 male mice were housed in the Laboratory Animal Care Facility at the Boston University on a 12 hour light/dark cycle. Food and water were given *ad libitum*. All animals were cared for and treated in accordance with the ARVO statement for the use of animals in ophthalmic and vision research and the IACUC at Boston University.

Intravitreal Injections

Animals were anaesthetized with a mixture of ketamine/xylazine (100 mg/kg/10 mg/kg) and kept on a 37°C heating pad at all times except for the 2–5 minutes required to perform the injection. While unconscious, a drop of the topical anesthetic tetracainehydrocholoride 0.5% (Phoenix Pharmaceuticals, St. Joseph, MO) was applied to each eye. The eyes were kept moist at all times by the application of Dry Eye Relief eye drops (CVS Pharmacy). For injections, a dissecting microscope was used to magnify the eyes. The microinjection assembly consisted of a pulled glass micropipette with a 10 μm tip attached to a 10 μl Hamilton microsyringe via plastic tubing. The entire system was filled with mineral oil to provide sufficient pressure for

the injection. The sclera was punctured just behind the limbus using a 26 gauge needle while applying gentle pressure around the eye socket to extrude the eye. A single crystal of fluorescein was dissolved in the viral suspension to provide a visual confirmation that virus was spreading throughout the vitreous during the injection. The micropipette was then inserted into the vitreous cavity through the initial puncture hole. Approximately 2 μl of AAV with a titer of 1×10^{13} genome copies/ml (gc/ml) in PBS was then injected into the vitreous and the micropipette was kept in the eye for about 1 minute to prevent backflow and allow the solution to diffuse through the vitreous humor. The right eye received an injection of AAVrh8 (n = 5) or AAVrh10 (n = 5) vectors (each with an AAV2 backbone) encoding EGFP, while for each virus group the left eye received a sham injection of saline (n = 3) or no injection (n = 2) for comparison.

Production of AAV

AAV vectors were produced essentially has described (Broekman *et al.*, 2006) by triple transfection of 293T cells followed by iodixanol-gradient centrifugation and anion-exchange chromatography purification. The AAVrh10 helper plasmid pAR-rh10 was generated by replacing the AAVrh8 Cap gene (GenBank sequence AY242997) in pAR-8 (Broekman *et al.*, 2006)with the AAVrh10 Cap gene (synthesized based on GenBank AY243015;Celtek Genes, Nashville, TN). The AAV2 vector genome encoding EFGP under the CBA promoter was previously described (Broekman *et al.*, 2006). Viral titers were determined as genomic copies (gc) per μl using the quantitative real-time PCR method described by Veldwijk et al. (2002).

Tissue preparation

The animals were sacrificed 4 weeks after injection by first being heavily anaesthetized using isoflurane gas followed by decapitation. Their eyes were immediately enucleated, the anterior chamber removed, and the remaining eyecups were placed in 4% paraformaldehyde for 90 minutes, cryoprotected in 30% sucrose, then embedded for cryosectioning in OCT embedding medium (TissueTek, Torrence, CA). Retinas were cryosectioned at a thickness of 14 μm. In addition, one animal for each viral vector was fixed by cardiac perfusion, and the brain was removed and cryosectioned as above to evaluate the presence of EGFP-expressing cells in the brain. Cryosectioned slices were then visualized for EGFP epifluorescence using an Olympus Fluoview 300 confocal microscope (Olympus, Melville, NY).

Immunocytochemistry

Cryosectioned retinal slices were rehydrated in 0.1 M phosphate buffer, pH 7.4(PB) and then incubated in 5% normal blocking serum for 2 hours. Slices were then incubated with one of the following primary antisera overnight in a humid chamber at 4°C diluted in PB with 0.3% Triton X-100 (PBTX): mouse anti-GFAP (1:1000, 3670, Cell Signaling Technology, Danvers, MA), mouse anti-PKC (1:100, 610107, BD Transduction Labs, San Jose, CA), rabbit anti-calbindin (1:100, Sigma). The slides were then washed 3 × 10 minutes in PB, and then incubated with a Cy5 or DyLight 649conjugated secondary antiserum (Jackson ImmunoResearch) for 2 hours, diluted1:500 in PBTX.Slides were then washed, cover-slipped and imaged using confocal microscopy as described above. In each case, omission of the primary antibody was used as a control for non-specific secondary antiserum binding.

Quantification of cellular transduction and evaluation of transduction efficiency

Image J image analysis software (http://rsbweb.nih.gov/ij/, Wayne Rasband, National Institute of Mental Health, Bethesda, MD) was used to convert images to inverted grayscale. The *z project* function of Image J was used to obtain a single image by collapsing a 10–12 μm thick

confocal optical stack and Corel Draw™ (Corel Corp., Ottawa, ON) was used to arrange and label the images.

Co-localization was determined by using the *colocalization* Image J plugin (http://rsb.info.nih.gov/ij/plugins/colocalization.html, Pierre Bourdoncle, Institut Jacque Monod, Paris, France). Briefly, the red channel for the immunocytochemistry and the green channel for the EGFP from the confocal stack were collapsed separately and each converted to 8-bit images. The plugin then found regions of co-localization after a threshold was chosen for the display value for each image. Two points were considered co-localized if their respective intensities were higher than the set threshold and if the ratio of their intensities was higher than the baseline ratio value. The threshold chosen was 100 arbitrary fluorescent units and the ratio baseline was 50%. The resultant 8-bit image showed the points of co-localization and was displayed as a separate image. The colocalization was confirmed by comparing the colocalization in single optical sections.

Quantitative analysis of transduction efficiency in the OPL was also done using Image J software. The OPL was marked as a region of interest (ROI) using the freehand selection method. To assure unbiased thresholding of the images, the threshold was assigned as the inflection point for the ROI of each collapsed 12-bit image. On a plot of arbitrary fluorescent units obtained from the confocal microscope versus the number of pixels in the ROI, the inflection point was computed as a point on the curve at which the tangent crossed the curve using a custom made Image J plug-in. Fluorescence units above this threshold were obtained for each region using the *ROI manager*. The mean arbitrary fluorescence units values obtained in this way were averaged for AAVrh8 and AAVrh10 respectively, then plotted using Microsoft Excel.

Results

AAVrh8 and AAVrh10 transduction following intravitreal injection

In order to determine the cellular tropism of AAVrh8 and AAVrh10 vectors in the mouse retina, intravitreal injections were performed in the eyes of adult mice using 2 μl of 1×10^{13}gc/μl of either serotype and transduction was evaluated after a 4 week incubation period. This was chosen based on a pilot study that we conducted where we injected 2–3 μl of AAVrh8 at ~1×10^{10}gc/μl and assessed transduction efficiency at 3, 4, 5, 8 and 9 weeks after injection. We found cell transduction patterns were similar across all time points and decided to use 4 weeks for both AAVrh8 and AAVrh10 to ensure optimal transduction.

Transduction in the GCL and INL was generally patchy but found throughout the retina for both serotypes. AAVrh8 transduced presumptive amacrine cells in the lower third of the INL based on their location and morphology (Figure 1A). There were also transduced Müller cells, which were identified based on their columnar morphology and their projections through the ONL to the outer limiting membrane (OLM; Figure 1A). The outer plexiform layer (OPL) had transduced horizontal cells in the upper third of the INL (Figure 1A). There was also EGFP expression in a mixed population of apparent retinal ganglion cells (Figures 1A, 1B and 1C).

AAVrh10 transduction was similar to AAVrh8, however there were more EGFP expressing cells near the center of the INL with apparent processes that resembled bipolar cells in location and morphology (Figure 1E). Comparison of the EGFP with the rod bipolar cell marker PKCa in double-label experiments found no co-localization (data not shown). In addition, intravitreal injection of AAVrh10 appeared to transduce retinal pigment epithelium and some photoreceptors (Figure 1E). There was also EGFP in horizontal cells and the OPL, similar to the transduction seen with AAVrh8, but EGFP expression in horizontal cells with AAVrh10

appeared much more robust than with AAVrh8 (Figures 1C and 1E). With AAVrh10-EGFP, the expression in horizontal cells was often extensive, spanning the entire retina (Figure 1F).

Evaluation of horizontal cell transduction

We used immunocytochemistry for calbindin, which is a mouse horizontal cell marker (Peichl and Gonzalez-Soriano, 1994), to confirm that the EGFP expression in the OPL was in horizontal cells. We found that calbindin-immunoreactivity (-IR) co-localized with EGFP in the OPL for both AAVrh8 and AAVrh10, indicating that both serotypes were transducing horizontal cells (Figure 2).

In general, the intensity of EGFP appeared consistent between many cells transduced by AAVrh8 and AAVrh10. The main exception was in the OPL where the EGFP appeared much stronger with AAVrh10 than AAVrh8. We compared the transduction levels in the OPL by quantifying the amount of EGFP expressed (as mean fluorescence) in the OPL for each serotype. The level of fluorescence was ~3.5 fold higher in the OPL transduced with AAVrh10 than with AAVrh8, suggesting increased transduction efficiency (Figure 3).

The comparison of retinal cell transduction in the GCL, ONL and additional cells in the INL was not possible because of regional variation between retinal cryosections. While the horizontal cells were consistent throughout a transduced retina, the number of other transduced cell types varied regionally depending on the 14 μm cyosection being examined. This suggests that the horizontal cells were transduced more evenly throughout the retina, while other cell types were more regionally transduced within the retina.

Increased Müller cell GFAP expression was associated with viral transduction

Retinal Müller cells express increased levels of GFAP in response to retinal stress (Eddleston and Mucke, 1993; Honjo et al., 2000; Larsen and Osborne, 1996; Xue et al., 2006). Therefore, we evaluated retinal stress in the transduced retinas by comparing GFAP-IR in both transduced and non-transduced areas of the same retina and also in control retinas. We found increased GFAP-IR in areas that were expressing EGFP for both AAV serotypes (Figures 4A and 4B). Basal levels of GFAP were seen in transduced retinas in areas not expressing EGFP (Figures 4A and 4B). We also evaluated if EGFP was seen in the control eye or brains of injected animals. We found no evidence of increased EGFP in control retinas (Figure 4C) or in brain sections (not shown).

Discussion

Our current study demonstrated that both AAVrh8 and AAVrh10 vectors can strongly transduce cells in the INL. Other more widely used AAV serotypes, such as AAV2 vectors have shown the most promise for transducing cells in the GCL and ONL(Allocca et al., 2006; Martin et al., 2002; Surace and Auricchio, 2008), while serotypes such as AAV8 (AAV vectors with an AAV2 genome and AAV8 capsid) have shown some ability to transduce cells in the inner retina (Lebherz *et al.*, 2008). AAV2 vectors have previously shown the most promise for transducing cells in the GCL and ONL.AAVrh8 appeared to transduce amacrine cells particularly well, based on the location and morphology of the labeled cells. However, AAV2 has also been shown to efficiently transduce amacrine cells (Lebherz *et al.*, 2008). Both AAVrh8 and AAVrh10 were able to transduce presumptive bipolar cells, also based on their location and morphology. However, we did not find any co-labeling with PKCa-IR, a rod bipolar cell marker, and therefore they were probably cone bipolar cells.

Perhaps the most interesting finding was that both AAVrh8 and AAVrh10 robustly transduced horizontal cells, and particularly with AAVrh10 the transduction appeared to span the entire

OPL. Recent work by Dalkara et al, (2009) suggests that the inability of many AAV vectors to effectively transduce the inner retina from an intravitreal injection is due to the barrier created by the inner limiting membrane (ILM). However, our results suggest that at least the AAVrh8 and AAVrh10 serotypes can efficiently transduce beyond the GCL without any obvious barriers. Quantitative analysis of the intensity of EGFP suggested that AAVrh10 transduced horizontal cells nearly 3.5 fold better than AAVrh8. This suggests an interesting opportunity to selectively target horizontal cells. Since both serotypes did not exclusively transduce horizontal cells, additional specificity may be obtained by using horizontal cell-specific promoters, such as connexin 57 (Janssen-Bienhold et al., 2009). However it should be noted that EGFP expression beyond horizontal cells was inconsistent depending on the retinal region observed. Therefore, use of these viral vectors for other neuronal cell types may be useful to study local connections and environments, but may not be useful to transduce the retina as a whole beyond the horizontal cells.

The receptors for AAVrh8 and AAVrh10 are not yet known, but since both have similar cellular tropism, they may share some cell-surface receptor preference. Indeed, there are many other factors that affect AAV transduction, such as intracellular trafficking to the nucleus, decapsidation, and conversion of the single stranded DNA genome to double stranded DNA (Ding et al., 2005). Since both vectors used the same promoter and an AAV2 backbone, the slight differences in cellular tropism and the large difference in horizontal cell transduction may reflect properties conferred by their respective capsids. For instance, the differences in the capsid proteins might allow multiple viruses to tranduce individual cells because there could be a cellular difference in the density of cell surface receptors for different AAV capsids. It is also possible that differences in the viral ssDNA sequences could allow for faster conversion to dsDNA and elevated transgene expression.

Our study focused only on the transduction of the mouse retina over the course of 4 weeks, which was determined as a reasonable incubation time based on our initial pilot study. Previous studies have shown recombinant AAV vectors, such as AAV5 reaches its peak transduction at 5 weeks, however AAV2 may take up to 15 weeks (Auricchio et al., 2001; Yang et al., 2002). A more recent study in retina shows that AAV1, 4, 5, 7, 8 and 9 all reach their peak transduction efficiency by 2 weeks and AAV2 by 3 weeks (Lebherz *et al.*, 2008). Considering that AAV mediated transgene expression remains stable for years in rodent and primate retina (Lebherz et al., 2005; Riviere et al., 2006), we decided to conduct our experiments at 4 weeks post-injection, after most AAV serotypes would have reached their peak transduction in retina (Lebherz *et al.*, 2008). This was also consistent with our pilot study, which showed a nearly identical transduction pattern from 3–9 weeks post-injection. We also felt that 4 weeks reflected a reasonable time point for short-term neurochemical studies involving such techniques as gene knockdown by RNAi. However, we cannot discount the possibility that transduction efficiency may have increased over a longer incubation and future experiments should assess AAVrh8 and AAVrh10 over prolonged periods of time.

The increase in GFAP-IR levels in transduced areas of AAVrh8 and AAVrh10 was disconcerting but not totally disappointing. Some areas of the same transduced retinas did not show any evidence of GFAP elevation or stress, even if there were some EGFP positive cells, indicating that it was a localized phenomenon. This could have been due to mechanical damage from the injection, however we saw no evidence of retinal damage and the increased GFAP expression was apparent throughout large transduced areas of the retina that were not associated with the injection site. Further neurochemical tests could be done to determine if the retinal areas with elevated GFAP expression were functioning normally. It would also be useful in future studies to look for microglial activation in response to the viral transduction by using immunocytochemistry to look for evidence of microglial activation using markers such as CD11b or CD45(Santos et al., 2010). Additional tests should also be done to determine if the

high viral titer or the EGFP itself caused the stress response. However, EGFP has been used extensively in retina with AAV and it was not previously found to be toxic (Lebherz et al., 2008; Petrs-Silva et al., 2009; Rex et al., 2005).

We used relatively high viral titers (1×10^{13}gc/ml) and this could have contributed to the elevated GFAP expression. Indeed, our initial pilot study used ~1×10^{11}gc/μl and found a similar transduction pattern. We could also potentially use lower titers and obtain the same transduction pattern by developing self-complementary genomes. Wild-type AAV contains a single-stranded DNA genome which must be converted to double-stranded DNA in the host nucleus before its genes can be expressed. This is a rate limiting step for AAV transduction and can be overcome by using self complementary AAV vectors (McCarty, 2008). Infusion of these scAAV vectors in mouse retina yields a higher number of transduced cells and faster transgene expression kinetics at considerably lower vector doses (Natkunarajah et al., 2008; Yang et al., 2002). Also in a recent study, Petrs-Silva et al. (2009) demonstrated that scAAV vectors produced with AAV capsids carrying point mutations of different surface tyrosines (Y-F mutants), which were previously shown to be involved in the ubiquitination of AAV2 and subsequent targeting to proteosome degradation (Zhong et al., 2008), were exceptionally efficient in mouse retina at considerably lower doses than we used in the present study. The combination of scAAV vectors with Y-F mutants of AAVrh8 and AAVrh10 capsids (both carry highly homologous tyrosine residues) may yield new vectors with exceptional potency and broad applicability to probe the molecular biology of retina.

The results of this study showed that AAVrh8 and AAVrh10 are promising new candidates to better study the amacrine, horizontal and bipolar cells, all of which have been largely overlooked in previous studies relying on viral gene delivery to retina. While future work is needed to further optimize the use of these AAV vectors, their ability to transduce inner retina will undoubtedly make AAVrh8 and AAVrh10 promising candidates for gene delivery to the retina.

Acknowledgments

We would like to thank ZarminaKhankel and Felicitas B. Eldred for their technical assistance and JamitArgawal for the creation of the custom Image J plugin used in determining our thresholds for normalization. This research was supported by NIH EY004785 to W.D. Eldred.

Abbreviations

AAV	adeno-associated virus
EGFP	enhanced green fluorescent protein
gc	genome copies
GCL	ganglion cell layer
GFAP	glial fibrillary accessory protein
IACUC	Institutional Animal Care and Use Committee
ILM	inner limiting membrane
INL	inner nuclear layer
IPL	inner plexiform layer
-IR	immunoreactivity
LCA	Leber congenital amaurosis
OLM	outer limiting membrane

OPL	outer plexiform layer
PB	0.1 M phosphate buffer
PBTX	0.1 M PB saline with 0.3% Triton-X-100
PKC	protein kinase C
ROI	region of interest
RPE	retinal pigment epithelium
scAAV	self complimentary AAV

Reference List

Allocca M, Tessitore A, Cotugno G, Auricchio A. AAV-mediated gene transfer for retinal diseases. Expert Opin Biol Ther 2006;6:1279–1294. [PubMed: 17223737]

Auricchio A, Kobinger G, Anand V, Hildinger M, O'Connor E, Maguire AM, Wilson JM, Bennett J. Exchange of surface proteins impacts on viral vector cellular specificity and transduction characteristics: the retina as a model. Hum Mol Genet 2001;10:3075–3081. [PubMed: 11751689]

Bainbridge JW, Smith AJ, Barker SS, Robbie S, Henderson R, Balaggan K, Viswanathan A, Holder GE, Stockman A, Tyler N, Petersen-Jones S, Bhattacharya SS, Thrasher AJ, Fitzke FW, Carter BJ, Rubin GS, Moore AT, Ali RR. Effect of gene therapy on visual function in Leber's congenital amaurosis. N Engl J Med 2008;358:2231–2239. [PubMed: 18441371]

Bennicelli J, Wright JF, Komaromy A, Jacobs JB, Hauck B, Zelenaia O, Mingozzi F, Hui D, Chung D, Rex TS, Wei Z, Qu G, Zhou S, Zeiss C, Arruda VR, Acland GM, Dell'Osso LF, High KA, Maguire AM, Bennett J. Reversal of blindness in animal models of leber congenital amaurosis using optimized AAV2-mediated gene transfer. Mol Ther 2008;16:458–465. [PubMed: 18209734]

Broekman ML, Comer LA, Hyman BT, Sena-Esteves M. Adeno-associated virus vectors serotyped with AAV8 capsid are more efficient than AAV-1 or -2 serotypes for widespread gene delivery to the neonatal mouse brain. Neuroscience 2006;138:501–510. [PubMed: 16414198]

Cai X, Conley SM, Naash MI. RPE65: role in the visual cycle, human retinal disease, and gene therapy. Ophthalmic Genet 2009;30:57–62. [PubMed: 19373675]

Cearley CN, Wolfe JH. Transduction characteristics of adeno-associated virus vectors expressing cap serotypes 7, 8, 9, and Rh10 in the mouse brain. Mol Ther 2006;13:528–537. [PubMed: 16413228]

Cideciyan AV, Aleman TS, Boye SL, Schwartz SB, Kaushal S, Roman AJ, Pang JJ, Sumaroka A, Windsor EA, Wilson JM, Flotte TR, Fishman GA, Heon E, Stone EM, Byrne BJ, Jacobson SG, Hauswirth WW. Human gene therapy for RPE65 isomerase deficiency activates the retinoid cycle of vision but with slow rod kinetics. Proc Natl Acad Sci U S A 2008;105:15112–15117. [PubMed: 18809924]

Dalkara D, Kolstad KD, Caporale N, Visel M, Klimczak RR, Schaffer DV, Flannery JG. Inner Limiting Membrane Barriers to AAV-mediated Retinal Transduction From the Vitreous. Mol Ther. 2009

Dinculescu A, Glushakova L, Min SH, Hauswirth WW. Adeno-associated virus-vectored gene therapy for retinal disease. Hum Gene Ther 2005;16:649–663. [PubMed: 15960597]

Ding W, Zhang L, Yan Z, Engelhardt JF. Intracellular trafficking of adeno-associated viral vectors. Gene Ther 2005;12:873–880. [PubMed: 15829993]

Eddleston M, Mucke L. Molecular profile of reactive astrocytes--implications for their role in neurologic disease. Neuroscience 1993;54:15–36. [PubMed: 8515840]

Gao G, Alvira MR, Somanathan S, Lu Y, Vandenberghe LH, Rux JJ, Calcedo R, Sanmiguel J, Abbas Z, Wilson JM. Adeno-associated viruses undergo substantial evolution in primates during natural infections. Proc Natl Acad Sci U S A 2003;100:6081–6086. [PubMed: 12716974]

Grimm D. Production methods for gene transfer vectors based on adeno-associated virus serotypes. Methods 2002;28:146–157. [PubMed: 12413413]

Hauswirth WW, Aleman TS, Kaushal S, Cideciyan AV, Schwartz SB, Wang L, Conlon TJ, Boye SL, Flotte TR, Byrne BJ, Jacobson SG. Treatment of leber congenital amaurosis due to RPE65 mutations

by ocular subretinal injection of adeno-associated virus gene vector: short-term results of a phase I trial. Hum Gene Ther 2008;19:979–990. [PubMed: 18774912]

Honjo M, Tanihara H, Kido N, Inatani M, Okazaki K, Honda Y. Expression of ciliary neurotrophic factor activated by retinal Muller cells in eyes with. Invest Ophthalmol Vis Sci 2000;41:552–560. [PubMed: 10670488]

Inagaki K, Fuess S, Storm TA, Gibson GA, Mctiernan CF, Kay MA, Nakai H. Robust systemic transduction with AAV9 vectors in mice: efficient global cardiac gene transfer superior to that of AAV8. Mol Ther 2006;14:45–53. [PubMed: 16713360]

Jacobson SG, Boye SL, Aleman TS, Conlon TJ, Zeiss CJ, Roman AJ, Cideciyan AV, Schwartz SB, Komaromy AM, Doobrajh M, Cheung AY, Sumaroka A, Pearce-Kelling SE, Aguirre GD, Kaushal S, Maguire AM, Flotte TR, Hauswirth WW. Safety in nonhuman primates of ocular AAV2-RPE65, a candidate treatment for blindness in Leber congenital amaurosis. Hum Gene Ther 2006;17:845–858. [PubMed: 16942444]

Janssen-Bienhold U, Trumpler J, Hilgen G, Schultz K, Muller LP, Sonntag S, Dedek K, Dirks P, Willecke K, Weiler R. Connexin57 is expressed in dendro-dendritic and axo-axonal gap junctions of mouse horizontal cells and its distribution is modulated by light. J Comp Neurol 2009;513:363–374. [PubMed: 19177557]

Klein RL, Dayton RD, Leidenheimer NJ, Jansen K, Golde TE, Zweig RM. Efficient neuronal gene transfer with AAV8 leads to neurotoxic levels of tau or green fluorescent proteins. Mol Ther 2006;13:517–527. [PubMed: 16325474]

Larsen AK, Osborne NN. Involvement of adenosine in retinal ischemia. Studies on the rat. Invest Ophthalmol Vis Sci 1996;37:2603–2611. [PubMed: 8977474]

Lebherz C, Maguire A, Tang W, Bennett J, Wilson JM. Novel AAV serotypes for improved ocular gene transfer. J Gene Med 2008;10:375–382. [PubMed: 18278824]

Lebherz C, Maguire AM, Auricchio A, Tang W, Aleman TS, Wei Z, Grant R, Cideciyan AV, Jacobson SG, Wilson JM, Bennett J. Nonhuman primate models for diabetic ocular neovascularization using AAV2-mediated overexpression of vascular endothelial growth factor. Diabetes 2005;54:1141–1149. [PubMed: 15793254]

Maguire AM, Simonelli F, Pierce EA, Pugh EN Jr, Mingozzi F, Bennicelli J, Banfi S, Marshall KA, Testa F, Surace EM, Rossi S, Lyubarsky A, Arruda VR, Konkle B, Stone E, Sun J, Jacobs J, Dell'Osso L, Hertle R, Ma JX, Redmond TM, Zhu X, Hauck B, Zelenaia O, Shindler KS, Maguire MG, Wright JF, Volpe NJ, McDonnell JW, Auricchio A, High KA, Bennett J. Safety and efficacy of gene transfer for Leber's congenital amaurosis. N Engl J Med 2008;358:2240–2248. [PubMed: 18441370]

Martin KR, Klein RL, Quigley HA. Gene delivery to the eye using adeno-associated viral vectors. Methods 2002;28:267–275. [PubMed: 12413426]

McCarty DM. Self-complementary AAV vectors; advances and applications. Mol Ther 2008;16:1648–1656. [PubMed: 18682697]

Natkunarajah M, Trittibach P, McIntosh J, Duran Y, Barker SE, Smith AJ, Nathwani AC, Ali RR. Assessment of ocular transduction using single-stranded and self-complementary recombinant adeno-associated virus serotype 2/8. Gene Ther 2008;15:463–467. [PubMed: 18004402]

Pacak CA, Mah CS, Thattaliyath BD, Conlon TJ, Lewis MA, Cloutier DE, Zolotukhin I, Tarantal AF, Byrne BJ. Recombinant adeno-associated virus serotype 9 leads to preferential cardiac transduction in vivo. Circ Res 2006;99:e3–e9. [PubMed: 16873720]

Pawlyk BS, Smith AJ, Buch PK, Adamian M, Hong DH, Sandberg MA, Ali RR, Li T. Gene replacement therapy rescues photoreceptor degeneration in a murine model of Leber congenital amaurosis lacking RPGRIP. Invest Ophthalmol Vis Sci 2005;46:3039–3045. [PubMed: 16123399]

Peichl L, Gonzalez-Soriano J. Morphological types of horizontal cell in rodent retinae: a comparison of rat, mouse, gerbil, and guinea pig. Vis Neurosci 1994;11:501–517. [PubMed: 8038125]

Petrs-Silva H, Dinculescu A, Li Q, Min SH, Chiodo V, Pang JJ, Zhong L, Zolotukhin S, Srivastava A, Lewin AS, Hauswirth WW. High-efficiency transduction of the mouse retina by tyrosine-mutant AAV serotype vectors. Mol Ther 2009;17:463–471. [PubMed: 19066593]

Rabinowitz JE, Rolling F, Li C, Conrath H, Xiao W, Xiao X, Samulski RJ. Cross-packaging of a single adeno-associated virus (AAV) type 2 vector genome into multiple AAV serotypes enables transduction with broad specificity. J Virol 2002;76:791–801. [PubMed: 11752169]

Rex TS, Peet JA, Surace EM, Calvert PD, Nikonov SS, Lyubarsky AL, Bendo E, Hughes T, Pugh EN Jr, Bennett J. The distribution, concentration, and toxicity of enhanced green fluorescent protein in retinal cells after genomic or somatic (virus-mediated) gene transfer. Mol Vis 2005;11:1236–1245. [PubMed: 16402024]

Riviere C, Danos O, Douar AM. Long-term expression and repeated administration of AAV type 1, 2 and 5 vectors in skeletal muscle of immunocompetent adult mice. Gene Ther 2006;13:1300–1308. [PubMed: 16688207]

Santos AM, Martin-Oliva D, Ferrer-Martin RM, Tassi M, Calvente R, Sierra A, Carrasco MC, Marin-Teva JL, Navascues J, Cuadros MA. Microglial response to light-induced photoreceptor degeneration in the mouse retina. J Comp Neurol 2010;518:477–492. [PubMed: 20020538]

Surace EM, Auricchio A. Versatility of AAV vectors for retinal gene transfer. Vision Res 2008;48:353–359. [PubMed: 17923143]

Veldwijk MR, Topaly J, Laufs S, Hengge UR, Wenz F, Zeller WJ, Fruehauf S. Development and optimization of a real-time quantitative PCR-based method for the titration of AAV-2 vector stocks. Mol Ther 2002;6:272–278. [PubMed: 12349826]

Wang L, Calcedo R, Nichols TC, Bellinger DA, Dillow A, Verma IM, Wilson JM. Sustained correction of disease in naive and AAV2-pretreated hemophilia B dogs: AAV2/8-mediated, liver-directed gene therapy. Blood 2005;105:3079–3086. [PubMed: 15637142]

Xue LP, Lu J, Cao Q, Hu S, Ding P, Ling EA. Muller glial cells express nestin coupled with glial fibrillary acidic protein in experimentally induced glaucoma in the rat retina. Neuroscience 2006;139:723–732. [PubMed: 16458441]

Yang GS, Schmidt M, Yan Z, Lindbloom JD, Harding TC, Donahue BA, Engelhardt JF, Kotin R, Davidson BL. Virus-mediated transduction of murine retina with adeno-associated virus: effects of viral capsid and genome size. J Virol 2002;76:7651–7660. [PubMed: 12097579]

Zhong L, Li B, Mah CS, Govindasamy L, Agbandje-McKenna M, Cooper M, Herzog RW, Zolotukhin I, Warrington KH Jr, Weigel-Van Aken KA, Hobbs JA, Zolotukhin S, Muzyczka N, Srivastava A. Next generation of adeno-associated virus 2 vectors: point mutations in tyrosines lead to high-efficiency transduction at lower doses. Proc Natl Acad Sci U S A 2008;105:7827–7832. [PubMed: 18511559]

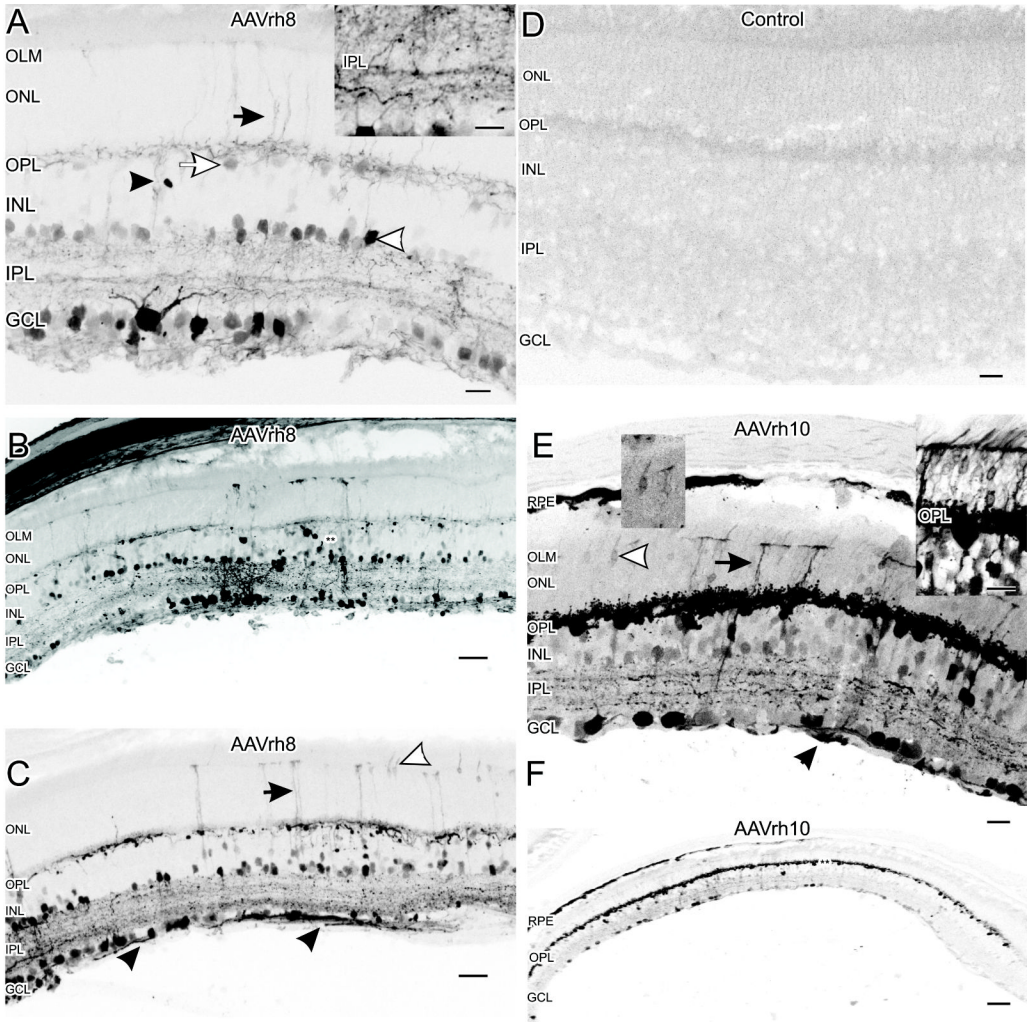

Figure 1.

Cellular tropism of AAVrh8 and AAVrh10 vectors in the mouse retina. (**A**) AAVrh8 transduced cells in the GCL and cells in the lower third of the INL (white arrowhead), which correspond to amacrine cells by location and morphology. While rare, some cells resembled bipolar cells by location and morphology (black arrowhead). There were apparent horizontal cell somata and processes in the OPL transduced with EGFP (white arrow). There were also processes from Müller cells extending up to the OLM (black arrow). Punctate EGFP expression, consistent with synapses, was also seen throughout the IPL. The inset (right) shows a higher magnification image with increased contrast to more clearly see the punctate expression in the IPL. Scale bars = 20 μm. (**B**) A lower magnification image of a retinal cross section transduced by AAVrh8 shows extensive regional labeling in the INL (double asterisks). Scale bar = 40 μm. (**C**) Consistent with ganglion cell transduction, there were EGFP-positive ganglion cell axons (black arrowheads). Müller cell processes can be seen projecting up to the OLM (black arrow) as well as some photoreceptor somata (white arrowhead). Scale bar = 40 μm. (**D**) Example of a control retina (sham injected with saline) with no EGFP. Scale bar = 20 μm. (**E**) EGFP levels were higher in retinas injected with AAVrh10. Transduction was seen in the GCL and throughout the INL. The OPL and apparent horizontal cells were strongly transduced with high levels of EGFP expression. There were also some labeled photoreceptor cell bodies (white arrowhead and insets) and Müller cells extending toward the OLM (black arrow). The inset directly above the white arrow shows a higher contrast image of the

photoreceptor indicated in the image. In inset right shows a high contrast image of a region of several transduced photoreceptors from a different retinal region. Some cells in the RPE also appeared transduced and EGFP-positive axons were seen in the GCL suggesting ganglion cell transduction (black arrowhead). Scale bar = 20 μm. (**F**) Typical transduction pattern for AAVrh10 showing extensive EGFP expression in the OPL (double asterisks) and more patchy expression in the inner retina. The overall AAVrh8 transduction pattern was similar to AAVrh10, but with less intense EGFP expression in the OPL and more regional expression in the inner retina (Figure 1B). Scale bar = 80 μm.

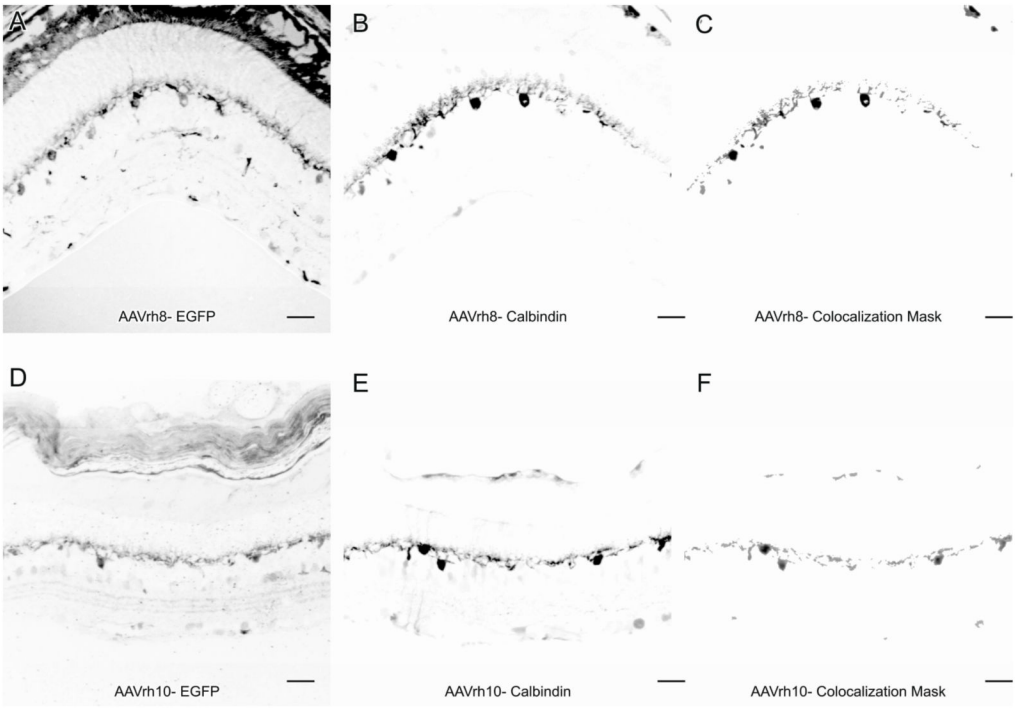

Figure 2.

AAVrh8 and AAVrh10 vectors transduce horizontal cells. EGFP from AAVrh8 and AAVrh10 transduction in the OPL co-localizes with the horizontal cell marker calbindin. Regions of co-localization as determined by the Image J *colocalization* plugin for AAVrh8 EGFP (**A**) and calbindin (**B**) are shown in (**C**). Regions of colocalization for AAVrh10 EGFP (**D**) and calbindin (**E**) are shown in (**F**). Scale bars = 20 μm.

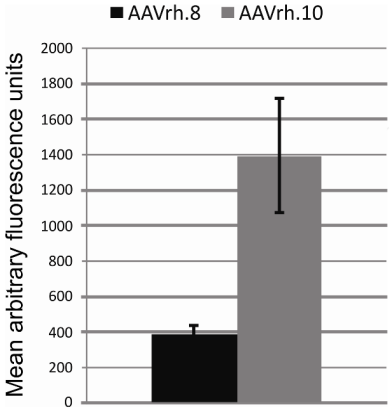

Figure 3.

Transduction in the OPL was stronger with AAVrh10 than with AAVrh8. Mean fluorescence of EGFP in the OPL was compared between the retinas of mice injected with AAVrh8 and AAVrh10. The mean fluorescence in the OPL in AAVrh10 transduced retinas was ~3.5 fold higher than in the OPL in AAVrh8 retinas. (*n*=5 per group) Error bars = SD.

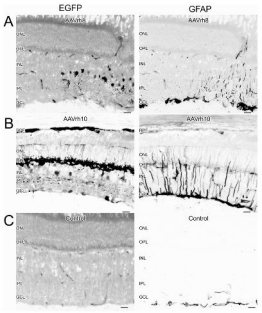

Figure 4.

Transduction with AAVrh8 and AAVrh10 vectors induced GFAP-IR expression in Müller cells. (**A**) GFAP-IR expression was seen in Müller cell processes in regions expressing EGFP from AAVrh8. (**B**) GFAP expression was also seen in Müller cell processes in regions expressing EGFP from AAVrh10. (**C**) Basal levels of GFAP were seen in the GCL of uninjected or sham-injected retinas, or in regions of the injected eyes not expressing EGFP. Scale bars = 20 μm.